Nonlinear Dynamics (2006) 43: 47–58

Symmetry, Optima and Bifurcations in Structural Design

PÉTER LÁSZLÓ VÁRKONYI[1,2] and GÁBOR DOMOKOS[1,3,*]

[1]*Department of Mechanics, Materials and Structures, Budapest University of Technology and Economics, Müegyeten RKP. 3, K242 H-1111 Budapest, Hungary;* [2]*Computer and Automation Research Institute of the Hungarian Academy of Sciences, Kende u. 13-17, H-1111 Budapest, Hungary;* [3]*Center for Applied Mathematics and Computational Physics, Budapest University of Technology and Economics, Budapest, Hungary;*

[*]*Author for correspondence (e-mail: domokos@iit.bme.hu; fax: +36-1-463-1773)*

(Received: 19 March 2004; accepted: 28 July 2004)

Abstract. Motivated by optimization problems in structural engineering, we study the critical points of symmetric, 'reflected', one-parameter family of potentials $U(p, x) = \max(f(p, x), f(p, -x))$, yielding modest generalizations of classical bifurcations, predicted by elementary catastrophe theory. One such generalization is the 'five-branch pitchfork', where the symmetric optimum persists beyond the critical parameter value. Our theory may help to explain why symmetrical structures are often optimal.

Key words: bifurcation, catastrophe theory, reflection symmetry, structural optimization

1. Introduction

Reflection symmetry can be observed in engineering structures as well as in nature and this suggests that reflection-symmetric configurations are often optimal. In case of many optimization problems we associate optima with minima, pessima with maxima of a potential. Symmetry-breaking bifurcations (studied extensively in [1]) associated with one-parameter families of smooth potentials $f(p, x)$ are adequate to model many problems in engineering; however, the classical pitchfork, associated with reflection-symmetric problems, predicts that the symmetric solution will become unstable beyond the critical parameter value, i.e. it will cease to be an optimal solution.

This prediction may be correct in some cases, but apparently not in each one: the symmetrical ($x = 0$) configuration of the three-hinged structure, illustrated in Figure 1A, proves to be (locally) optimal for all values of the parameter p if we are looking for maximal safety against buckling of the individual members (although there is a bifurcation if the optimal and pessimal values of x are plotted against p, *cf.* Figure 1B).

The discrepancy between the classical model's prediction and the actual behavior can be explained if we try to define a suitable 'potential' for the optimization problem. Consider that the global optimum is determined by a discrete assembly of 'weak points' the set of which, due to the reflection symmetry, is itself invariant under reflection. The potential associated with each of these 'weak points' behaves smoothly, but the envelope of these potentials will be, in general, non-smooth. In case of the three-hinged structure in Figure 1, we have two smooth potentials: $f(p, x)$ and $g(p, x)$ defined by

$$f(p,x) = \frac{N_1(x,\,p,\,N)}{N_1^{\mathrm{cr}}(x,\,p)} = \frac{l_1^2(x,\,p)}{\pi^2 EI} N_1(x,\,p,\,N) = \frac{N(1-x)}{2p\pi^2 EI}[p^2 + (1+x)^2]^{3/2} \tag{1}$$

$$g(p,x) = \frac{N_2(x,\,p,\,N)}{N_2^{\mathrm{cr}}(x,\,p)} = \frac{l_2^2(x,\,p)}{\pi^2 EI} N_2(x,\,p,\,N) = \frac{N(1+x)}{2p\pi^2 EI}[p^2 + (1-x)^2]^{3/2} \tag{2}$$

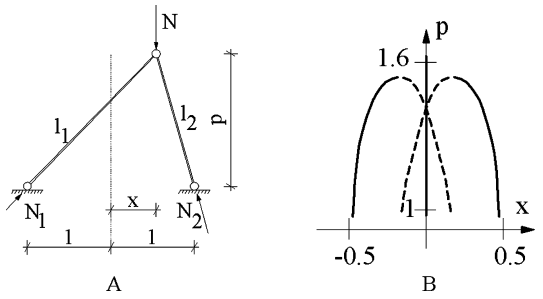

Figure 1. (A) A simple three-hinged model. (B) Optimization diagram (continuous line: optimum, dashed line: pessimum).

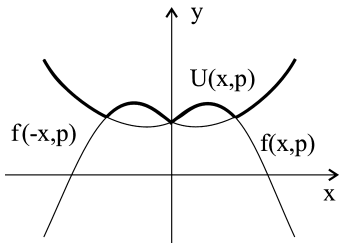

Figure 2. The reflected potential $U(x, p)$ at $p = 0.5$, generated *via* (3) from (1).

where N_1, N_2 denote the compressive forces in the members, N_1^{cr}, N_2^{cr} denote the corresponding Euler buckling loads. Observe that $g(p, x) = f(p, -x)$; the latter will be called the *generating potential* for the problem. The 'optimization potential' $U(p, x)$ of the structure can be generated from $f(p, x)$ as

$$U(p, x) = \max(f(p, x),\ f(p, -x)) \tag{3}$$

(see also Figure 2). It is easy to see that $U(p, x)$ has a (non-smooth) local minimum at $x = 0$ for almost all values of p; thus, this simple example *suggests* that the symmetric configurations are robust (non-smooth) optima in case of engineering structures.

In this paper, we take a systematic approach to the bifurcations associated with non-smooth potentials of type (3). Analysis of bifurcations associated with special non-smooth potentials can be found in [2, Section 16], where a generalization of Thom's theorem is introduced in case of the so-called *conditional* catastrophes; however, symmetrical potentials are not investigated.

The applications of classical catastrophe theory to engineering problems have been pioneered by Michael Thompson. In particular, the books with Giles Hunt [3, 4] serve as standard reference. We will follow the same line of thought, looking for the Taylor series expansion of the generating, smooth potential $f(p, x)$ at $x = 0$. This provides a classification of bifurcation points for the non-smooth optimization potential $U(p, x)$, containing both 'classical' cases as well as some new ones. The latter include bifurcations where the symmetrical solution remains stable (optimal) beyond the critical parameter value. Section 2 is devoted to the construction of this list, Section 3 provides structural engineering examples for each bifurcation. In Section 4 we summarize results and outline possible applications to mathematical models in evolution.

2. Reflected Potentials and the Associated Bifurcations

2.1. Critical Points of Reflected Potentials

We will investigate the class of 'reflected potentials' $U(x, p)$ defined in (3). At any constant value of p, these functions are at some isolated points $x = x_i$ not C^1 continuous (e.g. at $x = 0$, along the symmetry axis); thus, we need a generalized interpretation of critical points. Critical points of a smooth $f(x)$ function are the solutions of the $df/dx = f'(x) = 0$ equation. The first derivative $U'(x) = dU(x)/dx$ of reflected potentials $U(x, p)$ suffer discontinuities of the first kind at some isolated values $x = x_i$, i.e. the left-hand and right-hand limits $U'(x_i - 0, p)$ and $U'(x_i + 0, p)$ exist but are not identical. We apply the concept of *interval derivative* (see e.g. [5]) which is an interval $[U'(x_i - 0, p), U'(x_i + 0, p)]$. (For example, the interval derivative of $f(x) = |x|$ at $x = 0$ is the interval $[-1,1]$.) At smooth points, the interval derivative is a scalar, identical to the classical derivative. Using this concept, we call a point critical if the interval derivative contains 0 as an element.

2.2. Typical Bifurcations of Reflected Potentials

As already mentioned in Section 1, our goal is to give a local classification of one-parameter classes of reflected potentials $U(x, p)$ (defined in (3)), at $x = 0$; this is an analogue to Thom's theorem for smooth functions. The local classification of U can be reduced to the local classification of the smooth f generating potentials.

Thom's theorem shows that the local classification of a smooth function is determined by the lowest order non-vanishing term of the function's Taylor expansion. Let $T_f^{(n)}$ denote the truncated Taylor series of the function $f(x, p)$ up to the nth-order term.

At a general point on the p-axis ($x = 0$) $T_f^{(1)}$ does not vanish typically. At the same time, there exist typically a finite number of isolated points along the $x = 0$ line, where $T_f^{(1)}$ vanishes, and there is typically no point where $T_f^{(2)}$ vanishes.

If $T_f^{(1)}$ does not vanish, $f(x, p)$ is, according to Thom's theorem, locally equivalent of the (0, 0) point of the $f^{(1)}(x, p)$ function:

$$f^{(1)}(x, p) = x. \tag{4}$$

Consequently, the reflected $U(0, p)$ function generated from f *via* (3) is locally equivalent to the (0, 0) point of $U^{(1)}(x, p)$ generated from the $f^{(1)}$ potential in (4).

This type of point is analogous to non-degenerate critical points of smooth functions, but it is non-smooth (Figure 3).

If $T_f^{(1)}$ vanishes but $T_f^{(2)}$ does not, $U(0, p)$ is locally equivalent of $U^{(2)}$ (0, 0) generated from one of the following two $f^{(2)}$ functions:

$$f^{(2)}(x, p) = px \pm x^2 \tag{5}$$

The (0, 0) point of $U^{(2)}$ is analogous to a fold catastrophe point of a smooth functions. It has two dual forms: the unstable-X (Figure 4) and the point-like catastrophe (Figure 5). They appear different because the different role of maxima and minima in case of reflected functions. Figure 1B, associated with the three-hinged example, also shows an unstable-X type catastrophe point.

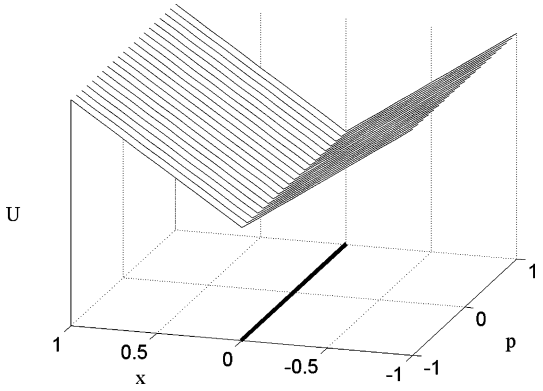

Figure 3. Non-degenerate critical point of reflected functions.

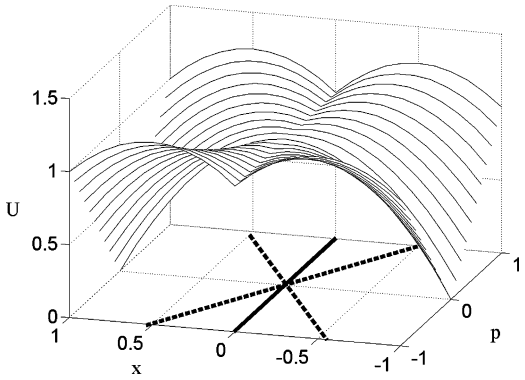

Figure 4. Unstable-X catastrophe.

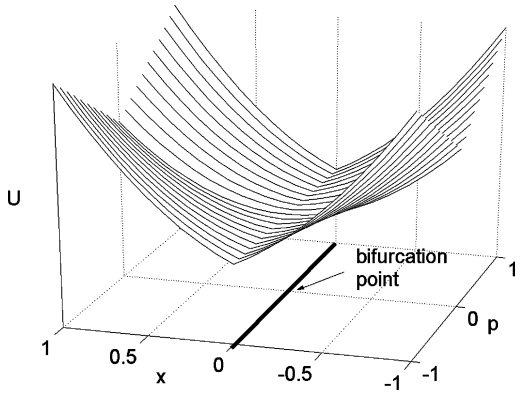

Figure 5. Point-like catastrophe.

As already introduced, higher degeneracy of $f(x, p)$ is atypical and there are no more typical catastrophes of one-parameter families of reflected functions. At the same time, there are applications, where $f(x, p)$ is, for some reason odd or even (the even or the odd terms of the Taylor expansion vanish). In these cases, some other catastrophes are typical.

In the case when $f(x, p)$ is odd, odd ($f(x, p)+c = -(f(-x, p)+c)$), typically there exist isolated points where U is locally equivalent of $U^{(3)}$ (0, 0) generated of $f^{(3)}$:

$$f^{(3)}(x, p) = px + x^3 \tag{6}$$

This corresponds to a 'five-branch pitchfork' (Figure 6) (which has no dual form).

In the case when $f(x, p)$ is even ($f(x, p) = f(-x, p)$), U is a smooth, symmetric function. The two emerging classes are well known: the first (typical) one is equivalent of $U^{(4)}$ (0, 0) generated of $f^{(4)}$

$$U^{(4)}(x, p) = f^{(4)}(x, p) = \pm x^2, \tag{7}$$

which is a one-dimensional Morse saddle, i.e. a smooth, non-degenerated critical point. Beyond this, there are typically isolated points where U is locally equivalent of $U^{(5)}$ (0, 0) generated of $f^{(5)}$:

$$U^{(5)}(x, p) = f^{(5)}(x, p) = px^2 \pm x^4 \tag{8}$$

These are the well-known standard and dual cusp catastrophe (Figure 7) points, producing the 'stable' and 'unstable' symmetric bifurcation. This is the typical bifurcation occurring in a one-parameter family of *symmetric, smooth functions*. In the following, this bifurcation will be called 'three-branch pitchfork'.

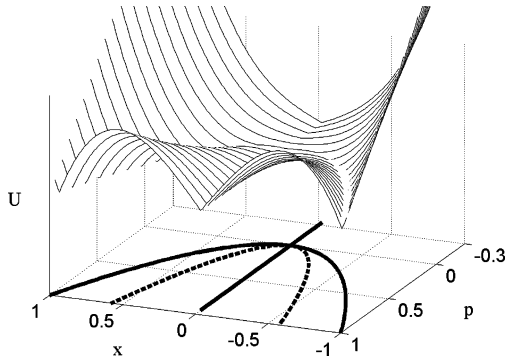

Figure 6. Five-branch pitchfork.

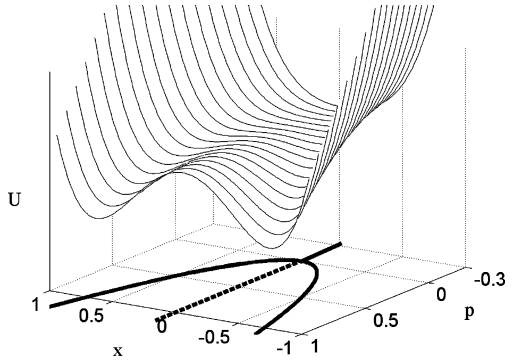

Figure 7. Standard cusp catastrophe, or stable three-branch pitchfork.

The presented catastrophes (5) and (6) have unusual properties. The most important is that $x = 0$ is *always* local optimum. This is completely atypical among smooth functions, it is true only at some degenerated bifurcations.

2.3. Multiple Reflected Potentials

There are many applications where the $\hat{U}(x, p)$ optimization potential is the envelope of several $U_i(x, p)$ reflected functions:

$$\hat{U}(x, p) = \max(U_i(x, p)), \quad i = 1, 2, \ldots, n, \tag{9}$$

where the functions $U_i(x, p)$ are defined by (3).

Among these functions, the typical bifurcations are the same as those of reflected potentials: the bifurcations of $\hat{U}$ are a subset of the bifurcations of the individual U_i functions. A bifurcation of U_k at $p = p_0$ appears in $\hat{U}$, if

$$U_k(0, p_0) = \max(U_i(0, p_0)). \tag{10}$$

In addition, one new type of bifurcation emerges: typically there are isolated V points at the $x = 0$ axis, where

$$U_i(0, p) = U_j(0, p), \quad i \neq j \tag{11}$$

At these points, a special 'wedge bifurcation' may appear (there is an example in Figure 8), typically if U_i has a local minimum, and U_j has a local maximum at V. (The latter can occur only for $U^{(4)}$ and $U^{(5)}$ type potentials.)

3. Examples in Engineering: Optimization of Structures

In this section, we provide a list of examples, illustrating all the bifurcations described in the previous section. Our goal was to make this illustration homogeneous and easy to follow in the sense that each bifurcation type is demonstrated on the *same type* of structure (continuous beam with four supports), as a result, some illustrations are somewhat artificial. Including a larger variety of structures yields other illustrations; however, their description is more lengthy. Similar examples have been studied in [6, 7].

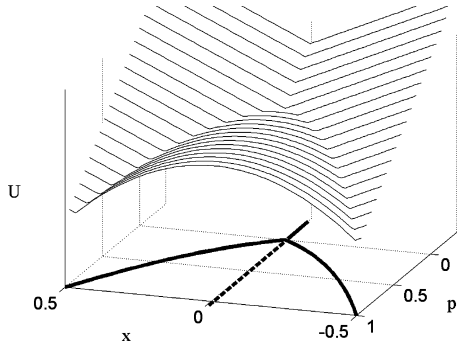

Figure 8. An example of the wedge bifurcation.

Load-bearing structures are designed based on *design conditions*, which have to be met by all parts or points of the structure. The most common examples are the strength conditions of the form

$$f \leq f_u, \tag{12}$$

where f and f_u are, respectively, the design and ultimate value of an internal force or stress. If the design variable x (describing the geometry of a structure together with the parameter p) is optimized for this kind of condition, it is plausible to define an 'optimization potential' $\hat{U}(x, p)$ as the maximum of $f(x, p)$ for all parts or points of the structure, a 'better' structure corresponding to smaller values of $\hat{U}(x, p)$.

Provided that:

- a one-parameter (p) family of structures is examined,
- $f(x, p)$ is a smooth function at all points or parts of the structure,
- x is a 'symmetrical' variable in the sense that there exists an x_0, such that $x = x_0 - c$ and $x = x_0 + c$ determine, at an arbitrary value of p, effectively the same but reflected structure,

$\hat{U}(x, p)$ is typically a 'multiple reflected potential' defined in (9).

In this section, we provide structures, the optimization of which produces the typical bifurcations of reflected potentials listed in Section 2. The variable x is symmetric in all examples with $x_0 = 0$ and all the introduced bifurcations appear at the p-axis of the x-p plane.

3.1. Unstable-X Bifurcation

Let us regard the uniform, linearly elastic beam in Figure 9A with four supports, subjected to uniform vertical load. Our goal is to optimism the position x of the hinge, making the maximum $\hat{U}$ of the bending moment as small as possible.

Calculating the support and hinge reactions under the assumption of small deformations (linear theory) is a common structural engineering problem. Solution techniques are available in advanced undergraduate textbooks; most easily it can be solved by the force method (*cf.* [8]), yielding finally the internal bending moment acting at an arbitrary point of the beam. The qualitative moment diagram is illustrated in Figure 9G. There are three pairs of local maxima in the moment diagram denoted by f_i and f_i'; $i = 1, 2, 3$. So $\hat{U}(x, p)$ is now the maximum of three pairs of local maxima (*cf.* (9)):

$$\hat{U} = \max(U_1, U_2, U_3), \tag{13}$$

where the U_is are reflected functions as defined in (3):

$$U_i = \max(f_i, f_i'), \quad i = 1, 2, 3 \tag{14}$$

In our example, the f_i functions can be determined analytically (*cf.* [8]) as:

$$f_2(x, p) = \frac{(p + x)[x + 4p(xp^2 + x^3 + (p - x)^3 + (p - x)^2)]}{8(p^3 + 3px^2 + p^2 + x^2)} \tag{15}$$

$$f_1(x, p) = \begin{cases} 1/2(1/2 - f_2(x, p))^2 & \text{if } f_2(x, p) \leq 1/2 \\ 0 & \text{if } f_2(x, p) > 1/2 \end{cases} \tag{16}$$

$$f_3(x, p) = \frac{1}{2}\left[x + \frac{f_2(-x, p) - f_2(x, p)}{2p}\right]^2 \tag{17}$$

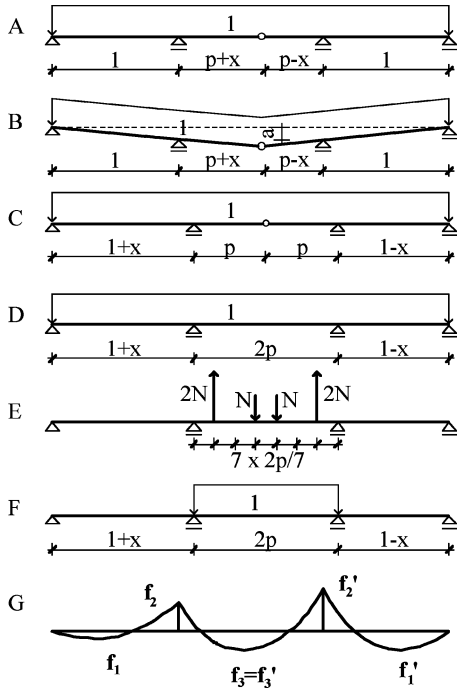

Figure 9. A–F: various parameterized beams and loads; G: qualitative moment diagram of the structures A–D.

We computed the catastrophe points of the U_i functions as the solutions of the $df_i(x, p)/dx = 0$ equation analytically and found the following results.

There is an unstable-X bifurcation in $U_2(x, p)$ at point

$$P = \left(0; \frac{1}{6}(19 + 3\sqrt{33})^{1/3} + \frac{2}{3}(19 + 3\sqrt{33})^{-1/3} - \frac{1}{3}\right) \approx (0, 0.420) \tag{18}$$

Since $U_2 > U_1$ at P, this X-bifurcation of U_2 occurs in the $\hat{U}$ function as well (*cf.* (10) and the corresponding remarks in Section 2.3). A representative domain of the bifurcation diagram is plotted in Figure 10. At point $V = (0, \sqrt{2} - 1)$ on the p-axis, we have $U_1 = U_2$, so we could expect a

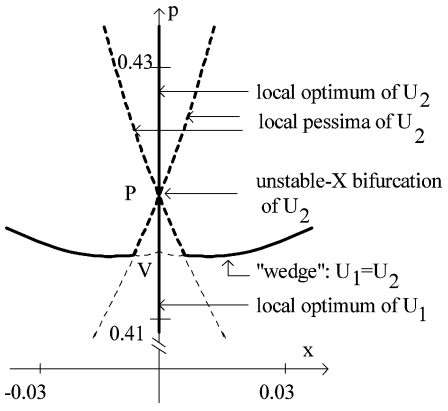

Figure 10. An example of the unstable-X bifurcation.

wedge bifurcation based on Equation (11). However, since both U_1 and U_2 have local minima at V, no bifurcation occurs (*cf.* comments after Equation (11)).

3.2. Point-Like Bifurcation

In Section 3.1, Equation (16) provides a simple relationship between f_1 and f_2 and it shows that the critical points of U_1 and U_2 typically coincide. Furthermore, the following form of (16) (where f_2^2 is approximated by its truncated Taylor expansion)

$$f_1(x, p) = \frac{\frac{1}{4} - f_2(x, p) + f_2^2(x, p)}{2} \approx \frac{\frac{1}{4} + f_2^2(0, p) - f_2(x, p)(1 - 2f_2(0, p))}{2} \tag{19}$$

shows that an unstable-X bifurcation point of U_2, corresponds to a dual, point-like bifurcation point of U_1 if $f_2(0, p) < 1/2$ (which is true for $p < 1$). So U_1 has a point-like bifurcation at $P \approx (0, 0.420)$ (*cf.* Figure 10); however, it is hidden because $\hat{U} \neq U_1$ at point P. In order to make the point-like bifurcation at P appear in $\hat{U}$, we change the geometry of the structure slightly.

The new geometry is illustrated in Figure 9B: the two inner supports are both symmetrically moved down by the distance a (this could be the result of soil settlement). This modification causes, according to our computations, the following effects:

– moves the critical point P downward in the bifurcation diagram,
– does not change the position of point V because the moment diagrams are unchanged if $x = 0$.

If, e.g. $a = 0.003$, the new bifurcation point P' is under V, and the point-like bifurcation of U_1 appears in $\hat{U}$ (Figure 11).

3.3. Five-Branch Pitchfork Bifurcation

The example of Figure 9C is similar to the previous ones, but the position of the middle supports is optimized instead of the position of the hinge. Analysis is done in the same way as at the first example.

The bending moment f_{mid} at the middle of the structure is zero at arbitrary (x, p) values, since there is a hinge. On the other hand, f_{mid} can be expressed from f_2 and f_2' as:

$$f_{\text{mid}} = (f_2 + f_2')/2 - p^2/2 \tag{20}$$

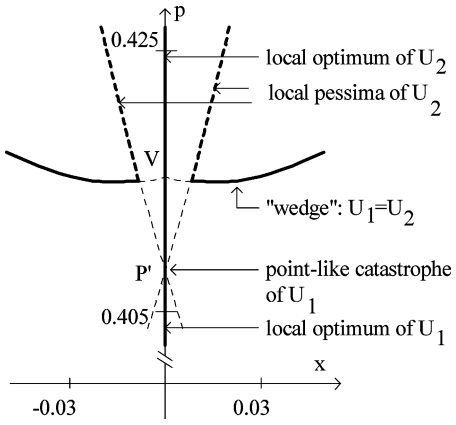

Figure 11. An example of the point-like bifurcation.

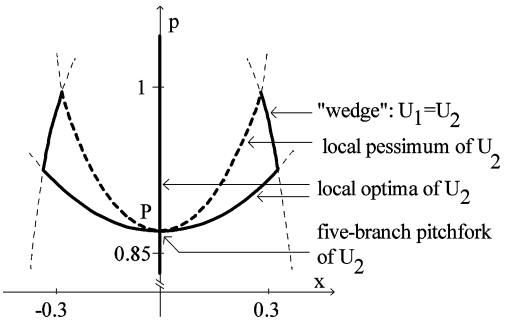

Figure 12. An example of the five-branch pitchfork.

Combining (20) with $f_{\text{mid}} = 0$ yields

$$p^2 = f_2(x, p) + f_2'(x, p) = f_2(x, p) + f_2(-x, p) \tag{21}$$

According to (21), f_2 is an odd function of x (the non-vanishing constant term does not influence the critical points), so at the bifurcation point $p = (0, \sqrt{3}/2)$ it is locally equivalent to $f^{(3)}$ (defined in (6)); thus, the bifurcation of U_2 is a five-branch pitchfork. In the neighborhood of P, $U_2 > U_1$, so, based on (10), this bifurcation occurs in $\hat{U}$ as well (*cf.* Figure 12.)

3.4. Three-Branch Pitchfork Bifurcation

The beam of Figure 9D is again slightly different of the previous ones: the hinge is missing. This structure is statically indeterminate of the second degree, so two compatibility equations are needed beyond the equilibrium equations. The solution is constructed in the same way as at the other examples.

As f_3 occurs at the symmetry axis of the structure, we have:

$$f_3(x, p) = f_3(-x, p) \tag{22}$$

and

$$f_3(x, p) = f_3'(x, p) = U_3(x, p) \tag{23}$$

Since U_3 is always a smooth, symmetric function of x, the typical bifurcation of U_3 is the (stable or unstable) three-branch pitchfork. In our example, U_3 has a stable pitchfork at point $P \approx (0, 0.4805)$. (The second coordinate of P has been computed numerically as a root of $f_3'' = 0$, leading to a sixth-order polynomial equation.) Since U_3 is not the global maximum of the bending moment at P, the structure has to be modified in order to have the pitchfork in $\hat{U}$ as well.

One example of such a modification is adding the loads of Figure 9E to the structure. This load has the following properties:

– It leaves the moment diagram in the outer spans invariant and only changes the moment diagram in the middle span: it increases U_3 and does not influence U_2 and U_1. If N is chosen appropriately, U_3 becomes global maximum.
– The effect of the load is independent of x, so the character of the bifurcation remains unchanged.

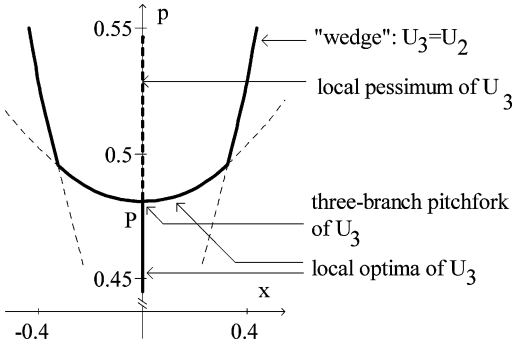

Figure 13. An example of the 'stable' three-branch pitchfork.

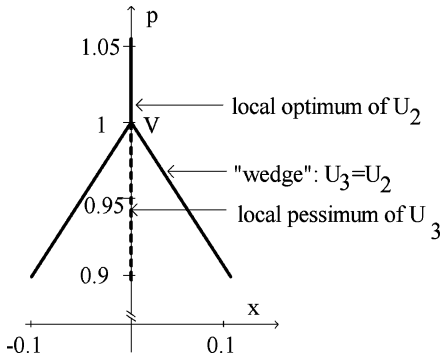

Figure 14. An example of the wedge bifurcation.

Figure 13 shows the bifurcation diagram for $N = 1$. At this value of N we can observe the 'stable' symmetric bifurcation in $\hat{U}$.

3.5. Wedge Bifurcation

Let us consider Figure 9F. The structure is the same as the one in Figure 9D; however, the load on the outer spans is now zero. At point $V = (0, 1)$ we have $U_2 = U_3$. At this point, U_2 has a local minimum and U_3 (which is a $U^{(4)}$ type potential, *cf.* (7)) has a local maximum. The two functions form a wedge bifurcation, which appears in $\hat{U}$. The corresponding bifurcation diagram is illustrated in Figure 14.

4. Summary

In this paper, we developed a modest generalization of classical bifurcations to model the optimization of engineering structures with reflection symmetry. Our basic observation was that an optimal shape is determined often by an assembly of several weak points. As a consequence, the associated potential can be obtained as a maximum of several smooth potentials, the resultant is a non-smooth function. Elementary catastrophe theory provides a full 'catalogue' of bifurcations associated with one-parameter, smooth potentials based on the truncated Taylor series expansion. Following the same line of thought, we developed a systematic description of the bifurcations associated with non-smooth, 'reflected' potentials.

The list of relevant bifurcations included the classical pitchfork as well as new types, such as the 'X' bifurcation or the five-branch pitchfork. Our study showed that in this class of one-parameter functions *the symmetric configuration is typically optimal* and this confirms the engineer's intuition. However, this does not imply that structural optimization problems always have a trivial (symmetric) solution. On one hand, globally several optima can co-exist and asymmetric ones are often superior to the symmetric solution. On the other hand, there exist structures, where the symmetric solution is a pessimum. We illustrated several types of structures and the associated optima. We believe that the perspective offered by bifurcation theory may be helpful in the understanding of optimization problems in engineering.

We can observe that symmetric solutions are optimal not just in case of engineering structures but in Nature as well. In evolutionary processes, the symmetric species may survive branching (produced by the presence of asymmetric mutants) and classical models [9] can not capture this phenomenon. Currently, we are investigating a model, based on [9], which predicts that symmetric species may survive evolutionary branching (Várkonyi, P., Domokos, G., Meszéna, G: Emergence of asymmetry in evolution. Adaptive Dynamics Workshop, Budapest, 2004).

Acknowledgments

The financial support of OTKA grant TS49885 and the Bolyai Research Fellowship is gratefully acknowledged.

References

1. Golubitsky, M., Stewart, I., and Schaeffer, D. G., *Singularities and Groups in Bifurcation Theory*, Vol. 1, Springer-Verlag, New York, 1982.
2. Poston, T. and Stewart, J., *Catastrophe Theory and Its Applications*, Pitman, London, 1978.
3. Thompson, J. M. T. and Hunt, G. W., *A General Theory of Elastic Stability*, Wiley, London, 1973.
4. Thompson, J. M. T. and Hunt, G. W., *Elastic Instability Phenomena*, Wiley, Chichester, 1984.
5. Korn, G. A. and Korn, T. M., *Mathematical Handbook for Engineers*, 2nd edn., McGraw-Hill, New York, 1968.
6. Buella, Cs., 'Structural design: Asymmetry analogies and catastrophes', in *Scientific Paper Presented at the Annual Students' Competition*, Technical University of Budapest, 2002.
7. Alkér, K., 'Asymmetry and optimum in structural design', in *Scientific Paper Presented at the Annual Students' Competition*, Technical University of Budapest, 2001.
8. Gere, J. M. and Timoshenko, S. P., *Mechanics of Materials*, 3rd edn., PWS-Kent, Boston, MA, 1990.
9. Geritz, S. A. H., Metz, J. A. J., Kisdi, É., and Meszéna, G., 'Dynamics of adaptation and evolutionary branching', *Physical Review Letters* **78**(10), 2024–2027.